Molecular Structure of *p*-Azoxyanisole, a Mesogen, Determined by Gas-Phase Electron Diffraction Augmented by ab Initio Calculations

Nobuhiko Kuze, Motoi Ebizuka, Hideo Fujiwara, Hiroshi Takeuchi, Toru Egawa, and Shigehiro Konaka*

Department of Chemistry, Faculty of Science, Hokkaido University, Sapporo 060-0810, Japan

Geza Fogarasi

Department of Theoretical Chemistry, Eötvös University, Budapest H-1518, Hungary

Received: November 25, 1997

As the first attempt to determine the gas-phase structure of molecules forming liquid crystals, the molecular structure of *p*-azoxyanisole (PAA, $CH_3O-C_6H_4-NO{=}N-C_6H_4-OCH_3$), a mesogen, has been studied by gas electron diffraction. A high-temperature nozzle was used to vaporize the sample. The temperature of the nozzle was about 170 °C. Structural constraints were taken from HF/4-21G(*) ab initio molecular orbital calculations on PAA. Vibrational amplitudes and shrinkage corrections were calculated from the harmonic force constants given by normal coordinate analysis. The structural model assuming four conformers well reproduced the experimental data. Five bond distances, six bond angles, and two dihedral angles were determined. Mean amplitudes were adjusted in five groups. The dihedral angles between the phenylene rings and the azoxy plane have been determined to be 11(26)° and 11(11)°, and these values are in agreement with those in the solid phase determined by X-ray diffraction within experimental errors. The conformation of the core of this mesogen is mainly ascribed to the interaction between the π-electrons of the azoxy group and the aromatic rings.

Introduction

The mechanism of the molecular ordering in the liquid-crystal phase is an interesting problem and it is believed that the molecular geometry is one of the factors to determine it. In this sense, it is supposed to be important to know about the geometrical structures of mesogens[1] in the gas phase, where no intermolecular interaction is present. However, no experimental investigation has been reported on the structures of mesogens in the vapor phase. Gas-phase electron diffraction (GED) is a powerful method to study the structure and conformation of free molecules. The principal purpose of the present work is to determine the gas-phase molecular structure of a mesogen by GED. As a target molecule, *p*-azoxyanisole (PAA) was chosen. This compound is a well-known and extensively studied mesogen[2,3] and forms a nematic phase between 117 and 137 °C.[2] As shown in Figure 1, PAA has a fairly rigid core which consists of two phenylene rings and an azoxy group (−NO═N−) linking them. In the core, the planes of aromatic rings and the linking unit are not necessarily on the same plane because of the internal rotation about C−N bonds, which are measured by dihedral angles $\phi_1(N_{10}N_9C_6C_5)$ and $\phi_2(N_9N_{10}C_{12}C_{17})$ (see Figure 1).

It is interesting to know how dihedral angles ϕ_1 and ϕ_2 differ in the crystal, liquid-crystal, liquid, and gas phases. The crystal structures of PAA determined by X-ray diffraction have been reported in the literature such as in refs 4 and 5, the latter of which is the most recent and precise. In the nematic phase, the dihedral angles of deuterized PAA have been determined with considerable ambiguities by deuterium nuclear magnetic resonance,[6−9] and therefore, these NMR studies have not clarified the conformation. In addition to the experimental

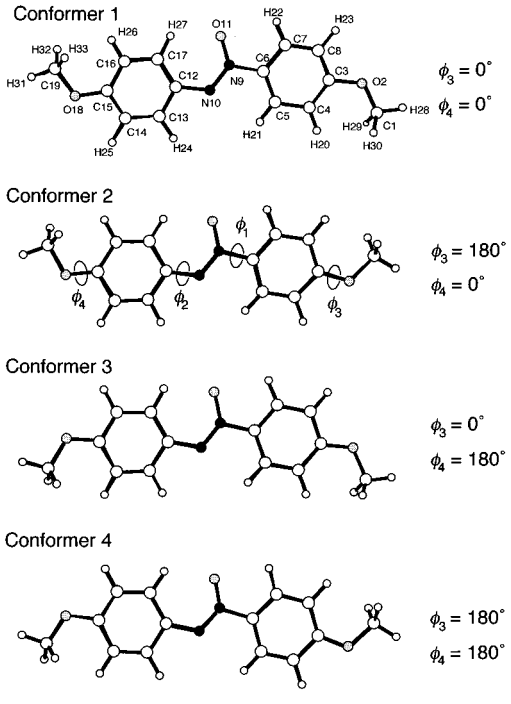

Figure 1. Four conformations with atom numbering of PAA. The four dihedral angles are $\phi_1(C_5C_6N_9N_{10})$, $\phi_2(N_9N_{10}C_{12}C_{17})$, $\phi_3(C_1O_2C_3C_4)$, and $\phi_4(C_{16}C_{15}O_{18}C_{19})$, respectively. Dihedral angle ϕ_1 is defined to be zero when the C_5-C_6 bond eclipses the N_9-N_{10} bond. When looking through C_6 toward N_9, its sign is positive if N_{10} rotates clockwise from the eclipsed position.

* Corresponding author.

S1089-5639(98)00321-1 CCC: $15.00
Published on Web 02/24/1998

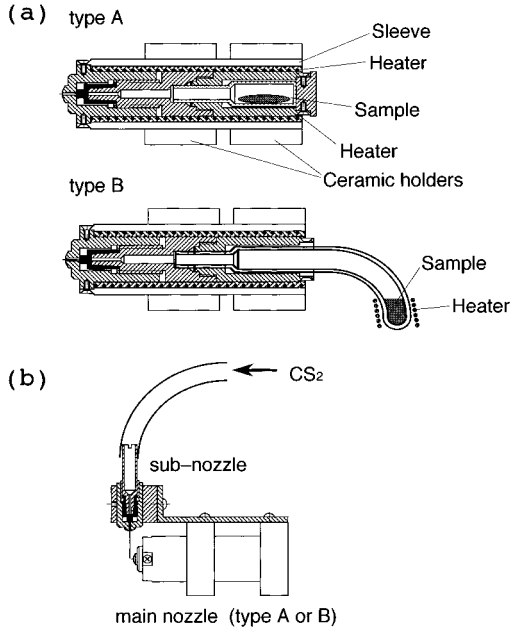

Figure 2. High-temperature nozzle: (a) cross sections of the two types of the main nozzle; (b) arrangement of the main nozzle and subnozzle.

investigations, some theoretical studies of molecular conformation have been carried out by means of semiempirical methods.[10−12] However, no complete set of the structural parameters has been reported.

A few difficulties exist in applying the GED method to PAA. First, this compound does not have enough vapor pressure to perform the GED experiment at room temperature. Therefore we made a high-temperature nozzle to heat the sample and took its diffraction patterns on photographic plates.

Second, PAA has too many interatomic distances which are closely spaced. Furthermore, the conformation can widely change by the internal rotation in the core and terminal substituents. Thus it is quite difficult to determine most of the structural parameters independently by GED alone. In such a system, quantum chemical calculations can be used to resolve structural parameters with certain accuracy. Therefore ab initio MO calculations were performed, and the results were used as constraints in the analysis.[13]

Third, the data analysis of PAA requires a very laborious and time-consuming work because of many structural parameters and vibrational modes.

Experimental Section

High-Temperature Nozzle. Figure 2a shows the cross sections of two high-temperature nozzles, A and B. Nozzle A was used at the short camera distance. The parts shaded in the figure were made of copper or stainless steel, which were heated by a silicon-rubber heater and worked as a heat bath. These parts were set in a sleeve made of stainless steel. The sample was placed in a glass holder of the nozzle.

At the long camera distance, a slightly revised setup, nozzle B, was used. In nozzle B, the sample holder was extended out of the sleeve and was heated separately from the nozzle by an additional heater. Thus the sample pressure could be controlled by this nozzle more easily than by nozzle A. Another advantage of this setup is that this sample holder can hold more sample than that of nozzle A. The temperature of nozzles A and B can be raised to about 200 °C.

Figure 2b shows the top view of the whole nozzle system. The direction of the electron beam is vertical to the paper.

TABLE 1: Experimental Conditions

	short	long
camera distance (mm)	244.5	489.4
nozzle temperature (K)	443	446
electron wavelength (Å)	0.06341	0.06352
uncertainty in the scale factor (%)	0.07	0.02
background pressure during exposure (10^{-6} Torr)	1−3	2−4
beam current (μA)	2.2	2.6
exposure time (s)	35−96	44−57
number of plates used	4	4
range of s value (Å^{-1})	6.3−33.7	2.1−17.4

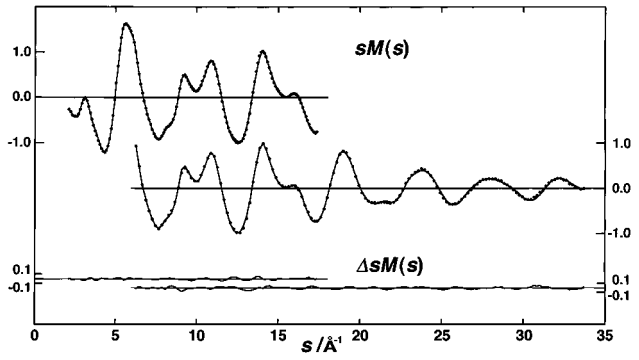

Figure 3. Experimental (···) and theoretical (−) molecular scattering intensities of PAA; $\Delta sM(s) = sM(s)^{obs} - sM(s)^{calc}$. The theoretical curve was calculated from the best fitting parameters.

Ceramic blocks were used to fix the main nozzle to the X−Y stage. The subnozzle fixed to the blocks was used to introduce the reference gas, CS_2, into the diffraction chamber at room temperature. In the present study, the subnozzle was heated by the third heater to prevent the sample effusing from the main nozzle, A or B, from depositing on the subnozzle tip.

Prior to the measurement of electron diffraction intensities, it was confirmed that the magnetic field generated by the heaters did not apparently affect the direction of the electron beam.

Gas Electron Diffraction. The sample of PAA with 98% purity (Aldrich Chemical Co. Inc.) was used without further purification. Electron diffraction patterns were recorded on Kodak projector slide plates in an apparatus equipped with an r^3-sector.[14] The temperature of the nozzle tip was measured to be about 170 °C by almel−chromel thermocouples. Exposure times were determined by measuring the current of scattered electrons. The diffraction patterns of CS_2 were recorded at 22−24 °C in the same sequence of exposures as the sample. The photographic plates were developed for 4.5 min in Dektol developer diluted 1:1. The accelerating voltage of incident electrons was about 37 kV, and the electron wavelength was calibrated by the known r_a(C═S) distance of CS_2 (1.5570 Å).[15] Other experimental conditions are summarized in Table 1.

Data reduction was made as described in ref 16, and leveled intensities were averaged for four plates at each camera distance. The total experimental intensities and backgrounds are available as Supporting Information. The experimental molecular scattering intensities are shown in Figure 3 with calculated ones in the final refinement. Elastic and inelastic atomic scattering factors were taken from literature.[17,18]

Theoretical Calculations

Ab initio molecular orbital (MO) calculations were performed with TX90 program system[19] employing the 4-21G(*) basis set[20,21] and empirical correction by offset forces.[21] The 4-21G(*) basis set is the original 4-21G basis set with a set of five d

TABLE 2: Optimized Geometric Parameters[a] and Relative Energies Calculated for PAA in the ab Initio MO Computations at the HF/4-21G(*) Level, Using Offset Forces[b]

	conformer 1	conformer 2	conformer 3	conformer 4		conformer 1	conformer 2	conformer 3	conformer 4
				Bond Lengths					
O_2-C_1	1.427	1.428	1.427	1.428	$C_{17}-C_{12}$	1.402	1.402	1.413	1.413
C_3-O_2	1.357	1.357	1.357	1.357	$C_{17}-C_{16}$	1.398	1.398	1.385	1.385
C_4-C_3	1.401	1.411	1.401	1.411	$O_{18}-C_{15}$	1.361	1.361	1.361	1.361
C_5-C_4	1.393	1.381	1.393	1.381	$C_{19}-O_{18}$	1.426	1.426	1.425	1.426
C_6-C_5	1.392	1.403	1.392	1.403	$H_{20}-C_4$	1.077	1.079	1.077	1.079
C_7-C_6	1.399	1.388	1.399	1.388	$H_{21}-C_5$	1.077	1.076	1.077	1.076
C_8-C_3	1.407	1.398	1.407	1.398	$H_{22}-C_7$	1.076	1.076	1.076	1.076
C_8-C_7	1.383	1.396	1.383	1.396	$H_{23}-C_8$	1.079	1.077	1.079	1.077
N_9-C_6	1.450	1.449	1.450	1.449	$H_{24}-C_{13}$	1.081	1.081	1.081	1.081
$N_{10}=N_9$	1.265	1.265	1.265	1.265	$H_{25}-C_{14}$	1.079	1.079	1.077	1.077
$O_{11}-N_9$	1.277	1.278	1.277	1.278	$H_{26}-C_{16}$	1.078	1.078	1.080	1.080
$N_{10}-C_{12}$	1.412	1.412	1.413	1.412	$H_{27}-C_{17}$	1.070	1.070	1.070	1.070
$C_{13}-C_{12}$	1.415	1.415	1.404	1.404	$H_{28}-C_1$	1.089	1.089	1.089	1.089
$C_{14}-C_{13}$	1.378	1.378	1.390	1.390	$H_{29}-C_1$	1.094	1.093	1.094	1.093
$C_{15}-C_{14}$	1.409	1.409	1.400	1.400	$H_{31}-C_{19}$	1.090	1.089	1.089	1.089
$C_{16}-C_{15}$	1.395	1.395	1.404	1.404	$H_{32}-C_{19}$	1.094	1.094	1.094	1.094
				Bond Angles					
$C_3-O_2-C_1$	117.6	117.5	117.6	117.5	$C_{17}-C_{12}-N_{10}$	129.5	129.5	129.4	129.4
$C_4-C_3-O_2$	125.2	115.3	125.2	115.3	$C_{17}-C_{12}-C_{13}$	118.0	118.0	117.9	118.0
$C_5-C_4-C_3$	120.0	120.7	120.0	120.7	$C_{17}-C_{16}-C_{15}$	120.8	120.8	121.5	121.5
$C_6-C_5-C_4$	120.1	119.5	120.1	119.5	$C_{16}-C_{17}-C_{12}$	120.5	120.5	120.0	120.0
$C_7-C_6-C_5$	120.3	120.3	120.3	120.3	$O_{18}-C_{15}-C_{14}$	115.5	115.5	125.3	125.3
$C_8-C_3-O_2$	115.5	125.4	115.5	125.4	$O_{18}-C_{15}-C_{16}$	125.6	125.6	115.8	115.7
$C_8-C_3-C_4$	119.3	119.3	119.3	119.3	$C_{19}-O_{18}-C_{15}$	117.3	117.3	117.4	117.4
$C_8-C_7-C_6$	119.7	120.3	119.7	120.3	$H_{20}-C_4-C_5$	118.8	121.1	118.8	121.1
$C_7-C_8-C_3$	120.6	119.9	120.6	119.9	$H_{21}-C_5-C_6$	119.6	119.7	119.6	119.6
$N_9-C_6-C_5$	121.8	121.7	121.8	121.8	$H_{22}-C_7-C_6$	118.8	118.7	118.8	118.7
$N_9-C_6-C_7$	117.9	118.0	117.9	118.0	$H_{23}-C_8-C_7$	121.1	118.9	121.1	118.9
$N_{10}=N_9-C_6$	115.4	115.4	115.4	115.3	$H_{24}-C_{13}-C_{12}$	118.2	118.2	118.2	118.2
$O_{11}-N_9-C_6$	116.2	116.3	116.2	116.3	$H_{25}-C_{14}-C_{13}$	121.5	121.5	119.2	119.2
$O_{11}-N_9=N_{10}$	128.3	128.3	128.4	128.4	$H_{26}-C_{16}-C_{17}$	118.2	118.2	120.5	120.5
$C_{12}-N_{10}=N_9$	120.0	120.0	120.0	120.1	$H_{27}-C_{17}-C_{12}$	119.7	119.7	119.7	119.7
$C_{13}-C_{12}-N_{10}$	112.6	112.6	112.6	112.6	$H_{28}-C_1-O_2$	105.6	105.6	105.6	105.6
$C_{14}-C_{13}-C_{12}$	121.6	121.6	122.2	122.1	$H_{29}-C_1-O_2$	111.4	111.4	111.4	111.4
$C_{15}-C_{14}-C_{13}$	120.1	120.1	119.5	119.5	$H_{31}-C_{19}-O_{18}$	105.7	105.7	105.7	105.7
$C_{16}-C_{15}-C_{14}$	119.0	119.0	119.0	119.0	$H_{32}-C_{19}-O_{18}$	111.5	111.5	111.5	111.5
				Dihedral Angles					
$C_4-C_3-O_2-C_1$	0.0[c]	180.0[c]	0.0[c]	180.0[c]	$H_{32}-C_{19}-O_{18}-C_{15}$	−61.3	61.3	61.4	−61.4
$C_{19}-O_{18}-C_{15}-C_{16}$	0.0[c]	0.0[c]	180.0[c]	180.0[c]	ΔE[d]	0.21	0.0	0.56	0.31
$C_3-O_2-C_1-H_{29}$	−61.4	61.4	61.4	−61.4					

[a] C_s symmetry was assumed. Bond lengths in angstroms, angles in degrees. Atom numbering is the same as shown in Figure 1. [b] Empirical offset forces are applied along the bond lengths during optimization to correct for systematic errors of the Hartree−Fock method; the offset forces for specific bond lengths were determined in a set of small reference molecules.[21] [c] Fixed values. [d] Relative energies in kcal mol^{-1}. The total energy computed for conformer 2 is −870.761 750 73 hartree.

functions of exponent 0.8 applied uniformly on atoms with lone pairs, i.e., nitrogen and oxygen atoms. The option of using empirical corrections on bond lengths, to correct for systematic errors of the Hartree−Fock method, is a special feature of TX90. The corrections are made by adding offset forces along bond-stretching coordinates to the ab initio potential surface during the optimization procedure. The offset values were determined in a set of small reference molecules.[21]

Four conformations of PAA shown in Figure 1 were optimized. C_s symmetry was assumed so that ϕ_1 and ϕ_2 are zero by symmetry. The $C_1O_2C_3C_4$ (ϕ_3) and $C_{16}C_{15}O_{18}C_{19}$ (ϕ_4) dihedral angles are (0°, 0°), (180°, 0°), (0°, 180°), and (180°, 180°). The resulting values of optimized structural parameters are listed in Table 2. The results reveal some geometrical properties: (1) the energies of the four conformers are in a narrow range of 0.6 kcal mol^{-1}; (2) fairly strong distortions of the structure of the phenylene rings are observed; (3) rotation of a methoxy group has only local effects, that is, it affects the ring to which it is attached, leaving the other ring unchanged; and (4) the geometry of the azoxy group shows no changes between the conformers.

Semiempirical MO calculations with AM1[22] and PM3[23] Hamiltonians were also carried out using the quantum mechanical program MOPAC version 6.01[24] on the Hewlett-Packard HP-705 running on a UNIX system. Geometry optimizations and calculations of the force constants were carried out because no force constants had been reported for PAA. The dihedral angles, (ϕ_1, ϕ_2), were obtained to be (18°, 2°) and (17°, 51°) for AM1 and PM3 calculations, respectively. Each methoxy group is coplanar with the phenylene ring to which it is attached.

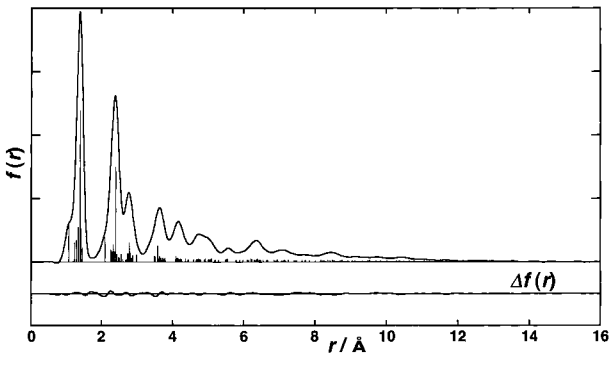

Figure 4. Experimental radial distribution curve of PAA; $\Delta f(r) = f(r)^{obs} - f(r)^{calc}$. Distance distributions are indicated by vertical bars.

TABLE 3: Mean Amplitudes and Interatomic Distances for PAA (Conformer 1)[a]

atom pair[b]	l_{calc}[c]	l_{obs}[d]	r_a[e]	i[f]	atom pair[b]	l_{calc}[c]	l_{obs}[d]	r_a[e]	i[f]
C−H_{ph}[g]	0.077	0.076(7)	1.072	1	$C_6\cdots C_{17}$	0.085	0.100	4.433	4
C−H_{OMe}[g]	0.079	0.077	1.087	1	$C_6\cdots C_{13}$	0.088	0.103	4.595	4
N_9-N_{10}	0.043	0.041	1.244	1	$C_8\cdots N_{10}$	0.078	0.093	4.672	4
N_9-O_{11}	0.043	0.041	1.302	1	$N_9\cdots C_{14}$	0.071	0.087	4.705	4
$C_{15}-O_{18}$	0.044	0.042	1.346	1	$C_4\cdots O_{11}$	0.075	0.091	4.746	4
O_2-C_3	0.044	0.042	1.349	1	$C_7\cdots C_{12}$	0.076	0.091	4.752	4
$C_{13}-C_{14}$	0.046	0.044	1.381	1	$C_1\cdots C_7$	0.069	0.084	4.767	4
C_7-C_8	0.047	0.045	1.386	1	$C_{13}\cdots C_{19}$	0.068	0.084	4.770	4
C_5-C_6	0.047	0.045	1.395	1	$C_5\cdots C_{13}$	0.137	0.152	4.786	4
C_4-C_5	0.047	0.045	1.396	1	$C_3\cdots N_{10}$	0.090	0.105	4.911	4
$C_{16}-C_{17}$	0.046	0.044	1.401	1	$C_3\cdots O_{11}$	0.087	0.102	4.934	4
C_6-C_7	0.047	0.045	1.402	1	$C_1\cdots C_6$	0.081	0.096	5.022	4
$C_{15}-C_{16}$	0.047	0.046	1.403	1	$C_{12}\cdots C_{19}$	0.080	0.095	5.036	4
C_3-C_8	0.047	0.045	1.403	1	$N_9\cdots C_{15}$	0.075	0.090	5.045	4
C_3-C_4	0.047	0.045	1.404	1	$O_{11}\cdots C_{14}$	0.114	0.129	5.112	4
$C_{12}-C_{17}$	0.048	0.047	1.405	1	$O_{11}\cdots C_{15}$	0.122	0.137	5.114	4
$C_{14}-C_{15}$	0.047	0.046	1.412	1	$C_5\cdots C_{17}$	0.114	0.129	5.193	4
$C_{12}-C_{13}$	0.048	0.047	1.418	1	$C_7\cdots C_{17}$	0.118	0.140(61)	5.311	5
C_1-O_2	0.049	0.047	1.419	1	$N_{10}\cdots O_{18}$	0.070	0.093	5.522	5
$O_{18}-C_{19}$	0.048	0.047	1.420	1	$C_4\cdots C_{12}$	0.105	0.127	5.534	5
$N_{10}-C_{12}$	0.047	0.046	1.428	1	$O_2\cdots N_9$	0.069	0.092	5.557	5
C_6-N_9	0.051	0.049	1.466	1	$C_6\cdots C_{16}$	0.084	0.107	5.798	5
$N_{10}\cdots O_{11}$	0.054	0.058(7)	2.272	2	$C_7\cdots C_{13}$	0.108	0.131	5.816	5
$C_6\cdots N_{10}$	0.063	0.066	2.292	2	$C_6\cdots C_{14}$	0.086	0.108	5.903	5
$O_2\cdots C_8$	0.059	0.063	2.304	2	$C_8\cdots C_{12}$	0.076	0.099	5.987	5
$C_{14}\cdots O_{18}$	0.059	0.063	2.324	2	$C_4\cdots C_{13}$	0.155	0.178	6.120	5
$N_9\cdots C_{12}$	0.056	0.060	2.331	2	$C_5\cdots C_{14}$	0.136	0.159	6.141	5
$N_{10}\cdots C_{13}$	0.064	0.067	2.348	2	$O_2\cdots O_{11}$	0.094	0.117	6.212	5
$C_6\cdots O_{11}$	0.062	0.065	2.371	2	$O_2\cdots N_{10}$	0.095	0.118	6.240	5
$C_{15}\cdots C_{19}$	0.058	0.062	2.389	2	$C_3\cdots C_{12}$	0.089	0.111	6.309	5
$C_1\cdots C_3$	0.059	0.062	2.393	2	$N_9\cdots O_{18}$	0.079	0.102	6.377	5
$C_6\cdots C_8$	0.055	0.059	2.396	2	$O_{11}\cdots O_{18}$	0.132	0.155	6.394	5
$C_4\cdots C_6$	0.055	0.059	2.404	2	$C_6\cdots C_{15}$	0.080	0.102	6.401	5
$C_{16}\cdots O_{18}$	0.058	0.061	2.407	2	$N_{10}\cdots C_{19}$	0.084	0.107	6.446	5
$C_{13}\cdots C_{15}$	0.054	0.058	2.411	2	$C_1\cdots N_9$	0.089	0.112	6.461	5
$C_{12}\cdots C_{16}$	0.055	0.059	2.415	2	$C_5\cdots C_{16}$	0.112	0.135	6.481	5
$C_3\cdots C_7$	0.055	0.058	2.416	2	$C_4\cdots C_{17}$	0.112	0.135	6.552	5
$C_3\cdots C_5$	0.055	0.058	2.416	2	$C_8\cdots C_{17}$	0.109	0.132	6.638	5
$C_{12}\cdots C_{14}$	0.055	0.059	2.422	2	$C_7\cdots C_{16}$	0.120	0.143	6.688	5
$C_{15}\cdots C_{17}$	0.054	0.058	2.429	2	$C_5\cdots C_{15}$	0.117	0.117	6.87	
$C_4\cdots C_8$	0.057	0.060	2.429	2	$C_8\cdots C_{13}$	0.119	0.119	6.95	
$C_5\cdots C_7$	0.056	0.060	2.435	2	$O_{11}\cdots C_{19}$	0.166	0.166	6.95	
$O_2\cdots C_4$	0.058	0.061	2.436	2	$C_1\cdots N_{10}$	0.125	0.125	6.97	
$C_{14}\cdots C_{16}$	0.056	0.060	2.438	2	$C_3\cdots C_{13}$	0.137	0.137	7.07	
$C_{13}\cdots C_{17}$	0.057	0.060	2.443	2	$C_7\cdots C_{14}$	0.107	0.107	7.08	
$C_7\cdots N_9$	0.060	0.064	2.450	2	$N_9\cdots C_{19}$	0.106	0.106	7.15	
$C_5\cdots N_9$	0.063	0.067	2.492	2	$C_3\cdots C_{17}$	0.097	0.097	7.17	
$N_{10}\cdots C_{17}$	0.058	0.061	2.566	2	$C_1\cdots O_{11}$	0.098	0.098	7.26	
$C_7\cdots O_{11}$	0.095	0.100(19)	2.749	3	$C_7\cdots C_{15}$	0.102	0.102	7.44	
$C_5\cdots N_{10}$	0.090	0.095	2.756	3	$C_4\cdots C_{14}$	0.157	0.157	7.48	
$C_3\cdots C_6$	0.061	0.065	2.764	3	$O_2\cdots C_{12}$	0.093	0.093	7.64	
$O_{11}\cdots C_{12}$	0.090	0.094	2.771	3	$C_6\cdots O_{18}$	0.084	0.084	7.73	
$C_{12}\cdots C_{15}$	0.060	0.065	2.786	3	$C_4\cdots C_{16}$	0.112	0.112	7.85	
$C_5\cdots C_8$	0.063	0.068	2.789	3	$C_8\cdots C_{16}$	0.110	0.110	8.02	
$C_4\cdots C_7$	0.063	0.068	2.798	3	$C_5\cdots O_{18}$	0.123	0.123	8.17	
$O_{11}\cdots C_{17}$	0.131	0.135	2.807	3	$C_4\cdots C_{15}$	0.127	0.127	8.24	
$C_{13}\cdots C_{16}$	0.063	0.068	2.812	3	$C_8\cdots C_{14}$	0.115	0.115	8.25	
$C_{14}\cdots C_{17}$	0.063	0.068	2.832	3	$O_2\cdots C_{13}$	0.152	0.152	8.36	
$C_{16}\cdots C_{19}$	0.089	0.093	2.858	3	$C_1\cdots C_{12}$	0.130	0.130	8.37	
$C_1\cdots C_4$	0.089	0.094	2.888	3	$C_3\cdots C_{14}$	0.134	0.134	8.42	
$N_9\cdots C_{17}$	0.080	0.084	2.994	3	$O_2\cdots C_{17}$	0.100	0.100	8.50	
$N_9\cdots C_{13}$	0.071	0.086(18)	3.496	4	$C_3\cdots C_{16}$	0.094	0.094	8.52	
$C_7\cdots N_{10}$	0.070	0.085	3.523	4	$C_6\cdots C_{19}$	0.106	0.106	8.56	
$O_2\cdots C_7$	0.062	0.077	3.582	4	$C_8\cdots C_{15}$	0.097	0.097	8.71	
$C_{13}\cdots O_{18}$	0.062	0.077	3.590	4	$C_7\cdots O_{18}$	0.113	0.113	8.76	
$C_1\cdots C_8$	0.065	0.081	3.598	4	$C_1\cdots C_{13}$	0.197	0.197	8.93	
$C_{14}\cdots C_{19}$	0.065	0.081	3.612	4	$C_3\cdots C_{15}$	0.103	0.103	9.06	
$C_5\cdots O_{11}$	0.071	0.087	3.619	4	$C_5\cdots C_{19}$	0.127	0.127	9.12	
$N_{10}\cdots C_{14}$	0.066	0.081	3.636	4	$C_1\cdots C_{17}$	0.126	0.126	9.33	
$C_6\cdots C_{12}$	0.066	0.081	3.640	4	$C_7\cdots C_{19}$	0.149	0.149	9.48	
$C_{17}\cdots O_{18}$	0.060	0.075	3.656	4	$C_4\cdots O_{18}$	0.135	0.135	9.53	
$O_2\cdots C_5$	0.060	0.075	3.676	4	$O_2\cdots C_{14}$	0.151	0.151	9.72	
$C_8\cdots N_9$	0.063	0.078	3.721	4	$O_2\cdots C_{16}$	0.096	0.096	9.85	

TABLE 3: (Continued)

atom pair[b]	l_{calc}[c]	l_{obs}[d]	r_a[e]	i[f]	atom pair[b]	l_{calc}[c]	l_{obs}[d]	r_a[e]	i[f]
$C_4\cdots N_9$	0.065	0.080	3.754	4	$C_8\cdots O_{18}$	0.105	0.105	10.03	
$N_{10}\cdots C_{16}$	0.061	0.077	3.799	4	$C_1\cdots C_{14}$	0.203	0.203	10.28	
$O_2\cdots C_6$	0.064	0.079	4.102	4	$C_3\cdots O_{18}$	0.108	0.108	10.38	
$C_8\cdots O_{11}$	0.097	0.113	4.117	4	$O_2\cdots C_{15}$	0.110	0.110	10.38	
$O_{11}\cdots C_{13}$	0.105	0.120	4.121	4	$C_4\cdots C_{19}$	0.131	0.131	10.49	
$C_{12}\cdots O_{18}$	0.064	0.079	4.122	4	$C_1\cdots C_{16}$	0.127	0.127	10.65	
$C_4\cdots N_{10}$	0.096	0.112	4.134	4	$C_8\cdots C_{19}$	0.135	0.135	10.79	
$O_{11}\cdots C_{16}$	0.134	0.149	4.153	4	$C_1\cdots C_{15}$	0.156	0.156	11.06	
$C_5\cdots C_{12}$	0.100	0.115	4.153	4	$C_3\cdots C_{19}$	0.112	0.112	11.25	
$N_{10}\cdots C_{15}$	0.066	0.081	4.195	4	$O_2\cdots O_{18}$	0.117	0.117	11.69	
$C_3\cdots N_9$	0.066	0.082	4.223	4	$C_1\cdots O_{18}$	0.168	0.168	12.35	
$C_{17}\cdots C_{19}$	0.091	0.106	4.240	4	$O_2\cdots C_{19}$	0.114	0.114	12.57	
$C_1\cdots C_5$	0.092	0.107	4.265	4	$C_1\cdots C_{19}$	0.151	0.151	13.30	
$N_9\cdots C_{16}$	0.080	0.096	4.367	4					

[a] Mean amplitudes and r_a distances are in angstroms. Atom numbering is shown in Figure 1. [b] Nonbonded atom pairs including hydrogen atom are not shown. $C-H_{ph}$ and $C-H_{OMe}$ denote the bonded atom pairs in phenylene and methoxy groups, respectively. [c] Calculated at 443 K. [d] Estimated errors of 3σ in the last significant digits are given in parentheses. [e] Taken from the final geometry. [f] The group of mean amplitudes (see text). [g] Average value.

Normal Coordinate Analysis

The infrared and Raman spectra of PAA have been investigated by several authors.[25−31] However, no spectral data are available in the gas phase. Thus, in the present study, we mainly referred to the observed spectra in the liquid phase. The observed frequencies and assignments were cited from the literature.[25,26,30] We also referred to the vibrational studies on related molecules, *trans*-azoxybenzene[32] and anisole.[33,34]

Cousseen et al.[35] suggested that the AM1 method is superior to the PM3 method for calculating rotational barriers in conjugated aromatic systems. Thus the force constants based on the AM1 calculation were used in the normal coordinate analyses. The elements of force constant matrix in local symmetry coordinates were modified so as to reproduce the observed vibrational frequencies by using the linear scaling formula.[36] The local symmetry coordinates, scale factors, scaled force constants, and the observed and calculated frequencies with potential energy distributions are available in the Supporting Information (Tables S2−S5 and Figure S1). In the region above 400 cm^{-1}, the calculated frequencies are in good agreement with the observed frequencies. The calculated frequencies differ from the observed ones by 1−13% in the region between 90 and 400 cm^{-1}. Below 90 cm^{-1}, there is no experimental data.

Structural Analysis

On the basis of the ab initio calculations, the following assumptions were made to reduce the number of adjustable parameters: (1) four different conformers (conformers 1−4 in Figure 1) coexist in the gas phase with the mole fractions of 26.0, 33.0, 17.6, and 23.4%, respectively, which were calculated from the energy differences obtained by the ab initio calculations; (2) the azoxy group takes a planar structure, that is, C_6, O_{11}, N_9, N_{10}, and C_{12} lie on the same plane; and (3) the differences between similar structural parameters are equal to those given by the ab initio calculations (see Table S6 in the Supporting Information for the details of the constraints). Adjustable structural parameters were thus taken to be r(C−H), $r(C-C)_{ring}$, r(N═N), r(C−N), r(N−O), ∠N═N−O, $\angle N_9{=}N_{10}-C_{12}$, $\angle N_{10}{=}N_9-C_6$, ∠N−C−C, $\angle CCC_{ring}$, ∠COC, ϕ_1, and ϕ_2. These structural parameters and the indices of resolution were determined by least-squares calculations on molecular scattering intensities, $sM(s)$.

Mean amplitudes and shrinkage corrections were calculated from the force constants obtained by normal coordinate analysis. The small amplitude vibrational model was adopted since no reliable potential functions for the C−N torsions are available. The anharmonicity constants, κ, of bonded atom pairs were estimated by the conventional method.[37,38] Those of nonbonded atom pairs were assumed to be zero. The mean amplitudes were divided into five groups and were refined by the same method as described in ref 16. Since similar distances existed in the nonbonded atom pairs and the corresponding peaks of the radial distribution (RD) curve overlapped with each other, the groups were selected according to the r_a distances such as (i) $r_a < 1.8$ Å, (ii) $r_a = 1.8-2.6$ Å, (iii) $r_a = 2.6-3.2$ Å, (iv) $r_a = 3.2-5.3$ Å, and (v) $r_a = 5.3-6.8$ Å. Group i contains the mean amplitudes of the bonded atom pairs in the first peak of the RD curve (see Figure 4). The grouping and the final r_a distances for conformer 1 are shown in Table 3, where the calculated and refined mean amplitudes are also listed. The final RD curve is shown in Figure 4, where atom pairs are indicated by vertical bars. The correlation matrix in the least-squares calculation is given in Table S7 of the Supporting Information.

Results and Discussion

Figures 3 and 4 show that the experimental data are well reproduced. This confirms the validity of the structural and conformational assumptions as well as the assumption of small amplitude vibrations adopted in the analysis. The observed geometry of PAA (conformer 1) determined by GED is listed in Table 4. The estimated errors listed in this table were calculated from 3 times the standard deviations of the least-squares analysis, and some of them may be somewhat optimistic. However, more precise error estimation is difficult at the present stage. In this table are also listed the geometry of PAA obtained by the ab initio MO calculation and that determined by X-ray diffraction[5] as well as the geometry of a related compound, *trans*-azobenzene (tAB, $C_6H_5-N{=}N-C_6H_5$),[39] obtained by GED.

1. Comparison between the Experimental and Theoretical Structures. The values of ϕ_1 and ϕ_2 determined by GED are 11(26)° and 11(11)°, respectively. The HF/4-21G(*) calculations assumed the existence of planar conformation for which $\phi_1 = \phi_2 = 0°$. The latter is a reasonable assumption in light of the GED results. A similar result ($\phi_1 = 18°$, $\phi_2 = 2°$) was obtained from the AM1 calculation. However, the result of PM3 calculation ($\phi_1 = 17°$, $\phi_2 = 51°$) is in poor agreement with the experimental one.

We could determine seven independent parameters of the interannular part of the molecule, which links the two phenyl

TABLE 4: Comparison of the Structural Parameters of PAA Determined by GED with the Geometry Obtained by ab Initio MO Calculations Including Empirical Corrections and with the Geometry Determined by X-ray Diffraction and Those of *trans*-Azobenzene (tAB) Obtained by GED[a]

	PAA			tAB[i]	
	GED[f]	ab initio[g]	X-ray[h]	GED[j]	GED[k]
		Bond Lengths			
$\langle C-H\rangle$[b]	1.083(6)	1.084		1.082(9)	1.088(9)
$\langle C_{me}-O\rangle$[b]	1.421	1.427	1.426(4)		
$\langle C_{ring}-O\rangle$[b]	1.350 (1)	1.359	1.351(4)		
$\langle C-C_{ring}\rangle$[b]	1.400	1.398	1.385(6)	1.396(3)	1.396(3)
$N_9=N_{10}$	1.245(12)	1.265	1.281(4)	1.259(12)	1.268(12)
N_9-O_{11}	1.303(12)	1.277	1.288(3)		
C_6-N_9	1.468	1.450	1.445(4)		
C12−N10	1.429 (13)	1.412	1.428(4)	1.420(12)	1.427(12)
		Bond Angles			
$N_{10}N_9O_{11}$	126.2(24)	128.3	124.6(3)		
$N_9N_{10}C_{12}$	122.4(19)	120.0	119.8(3)	116.0(12)	114.5(12)
$N_{10}N_9C_6$	115.8(21)	115.4	116.5(3)		
$N_9C_6C_5$	122.2 (10)	121.8	120.7(3)	121.2(15)	123.0(15)
$N_{10}C_{12}C_{17}$	130.0	129.5	127.5(3)	118.8	117.0
$\langle CCC_{ring}\rangle$[b]	120.0 (1)	120.0	119.9(3)		
$C_4C_3O_2$	124.8[c]	125.2	126.8(4)		
$C_{16}C_{15}O_{18}$	124.8[c]	125.6	126.1(4)		
$C_3O_2C_1$	122.7 (17)	117.6	119.4(2)		
$C_{15}O_{18}C_{19}$	122.5	117.3	119.1(2)		
		Dihedral Angles			
$C_5C_6N_9N_{10}$	11(26)	0	4.0(5)	30(5)	28(9)
$N_9N_{10}C_{12}C_{17}$	11(11)	0	18.2(5)		
$C_6N_9N_{10}C_{12}$	180[d]	180	180		
$C_1O_2C_3C_4$	0[d]	0	0		
$C_{16}C_{15}O_{18}C_{19}$	0[d]	0	−1		
$C_{12}N_{10}N_9O_{11}$	0[d]	0	0		
		Indices of Resolution[e]			
k (long)	0.972(12)				
k (short)	0.951(19)				

[a] Bond lengths in angstroms, angles in degrees. Estimated errors (3σ) in the last significant digits are given in parentheses. Errors are not listed for dependent parameters. Atom numbering is shown in Figure 1. [b] Average value. C_{me} and C_{ring} denote the carbon atoms of methoxy and phenylene groups, respectively. [c] Dependent parameter. [d] Fixed parameter. [e] The index of resolution, *k*, is defined as $sM(s)^{obs} = ksM(s)^{calc}$. [f] The structure of conformer 1 (r_g and $\angle_\alpha$). [g] The structure of conformer 1 obtained from the HF/4-21G(*) calculation (r_e) applying empirical corrections to bond lengths in form of "offset forces".[21] [h] Reference 5. [i] Two models are listed in ref 39 because it was not determined whether the phenyl groups rotated to the same or to the opposite side of the planar azo group around the C−N bonds. [j] Model with C_2 symmetry (r_a and $\angle_\alpha$). [k] Model with C_1 symmetry (r_a and $\angle_\alpha$).

rings, by the GED analysis. The calculated N=N and C−N distances at the HF/4-21G(*) level of theory agree moderately with the experimental ones. This calculation slightly overestimates the N=N distance and underestimates the N−O and C−N distances. The calculated values of N=N−O, N=N−C, and N−C−C angles are in good agreement with the experimental values. On the other hand, the calculation underestimates the C−O−C angles.

2. Comparison between the Structure of PAA and Those of Related Compounds. In Table 4, two structural models of tAB are listed since it had not been determined whether the phenyl groups rotate to the same or to the opposite side of the planar azo group around the C−N bonds.[39] This molecule has a nonplanar conformation in the gas phase where the phenyl groups twist around the C−N bonds by about 30°. The phenylene rings of PAA are less twisted from the plane of the central group than those of tAB. The bond distances of PAA are in agreement with the corresponding ones of tAB within the experimental errors. The experimental values of $N_9N_{10}C_{12}$ and $N_{10}C_{12}C_{17}$ angles are significantly larger than the corresponding ones of tAB, perhaps because of the interaction between the H_{27} atom and the O_{11} atom, which is absent in tAB.

The values of $C_{ring}-O$ and $C_{me}-O$ bond distances of PAA, 1.350(1) and 1.421(1) Å, agree well with the corresponding values of anisole,[40] 1.362(15) and 1.425(15) Å, and *p*-anisaldehyde,[41] 1.358(12) and 1.420(10) Å. Similarly the average value of COC angles of PAA, 122.6(17)°, is in good agreement with the corresponding values of anisole,[40] 120.0(20)°, and *p*-anisaldehyde,[41] 122.0(18)°. Thus the structure of each methoxy fragment changes slightly by the substitution to the *para* position of the aromatic ring.

The r(N−O) distance of PAA, 1.303(12) Å, is larger than the r(N=O) distances of aromatic nitro compounds, 1.22−1.24 Å,[42] and smaller than the r(N−O) distances of hydroxylamines, 1.39−1.51 Å.[41] This fact shows that the N−O bond of PAA has considerable double-bond character as mentioned by Exner et al.[43]

3. Comparison of the Conformations in the Vapor, Liquid-Crystal, and Solid Phases. The molecular conformation and orientational order of deuterized PAA in the nematic phase have been studied by NMR.[6−9] As described below, these studies gave various values for the dihedral angles, ϕ_1 and ϕ_2, depending on the different assumptions on the degree of the nonrigidity of molecular conformation. Dianoux et al.[7] determined the values of the dihedral angles of about 20°. In the study by Volino et al.,[9] a conformation of core was essentially unchanged from that in the solid. Dong et al.[6] pointed out that ϕ_1 and ϕ_2 appeared to be sensitive to temperature. The values of ϕ_2 at 128 and 107 °C determined by assuming $\phi_1 = 0°$ were found to be 60.1° and 37.3°, respectively. In comparison with these models, the change in the conformation of the core by going from the nematic phase to the gas phase is not clear.

The conformation of the methoxy groups in the gas phase is significantly different from that in the nematic phase.[7,9] Volino et al.[9] showed that the values of ϕ_3 and ϕ_4 were 32−40° under the assumption of the existence of a single stable conformer. In the gas phase, the present experimental data are consistent with the model of conformation in which two $C(H_3)-O$ bonds are on the same plane with the phenylene rings.

The ϕ_1 and ϕ_2 values of PAA in the crystal at 203 K were determined to be 4.0(5)° and 18.2(5)°, respectively.[5] Thus the conformation of the core in the vapor phase found in the present study is practically identical with that in the solid phase. This means that the influence of intermolecular interactions in crystal on molecular conformation is probably small. This conclusion leads a speculation that the conformation of PAA in the nematic phase is similar to those in the vapor and solid phases. In the crystalline state as well as in the gas phase, the repulsion between the H_{27} and O_{11} atoms makes the $N_{10}C_{12}C_{17}$ angle (127.5(3)°) larger than normal.

4. Conformation of the Aromatic Core. The conformation of the core of PAA is mainly determined by the following four factors: (1) the repulsive and attractive interactions between the H_{27} and O_{11} atoms; (2) the repulsive interaction between the ortho hydrogen atom, H_{21}, and the lone-pair electrons of nitrogen, N_{10}; (3) the interaction between the π-electrons of the azoxy group and the aromatic rings ($\pi-\pi$ interaction); and (4) the interaction between the nitrogen lone-pair electrons and the π-electrons of the rings (n−π interaction).

The tAB molecule has a nonplanar conformation in the gas phase. Traetteberg et al.[39,44] suggested that the nonplanarity of tAB might be explained by factors 2 and 4. The present study

shows that PAA has the phenylene rings that are less twisted from the plane of the central group than those of tAB. This conformational character of PAA can be explained by assuming that the contribution of the factor 3, which is maximized for the planar conformation, is larger than the contributions of other interactions. This assumption is quite reasonable considering that not only the N═N bond but also the N−O bond with the double-bond character can contribute to the $\pi-\pi$ interaction.

Conclusion

The gas-phase molecular structure and conformation of typical mesogen, PAA, have been determined by electron diffraction combined with ab initio calculations and vibrational spectroscopy. The dihedral angles between the aromatic rings and the interannular plane, ϕ_1 and ϕ_2, are 11(26)° and 11(11)°, respectively. This conformational property of PAA is mainly explained by the conjugation between the rings and the azoxy group. The double-bond character of the N−O bond contributes to the electron delocalization between them. The gas-phase conformation of PAA is similar to that in the crystal phase, showing that crystal packing has a limited effect on the conformation.

Acknowledgment. Data analysis was performed using the Hitac Models M-880 and S-820/80 at the Hokkaido University Computing Center.

Supporting Information Available: The leveled total intensities and the backgrounds (Table S1), the local symmetry coordinates (Table S2 and Figure S1), the scale factors for force constants (Table S3), scaled force constants (Table S4), the observed and calculated frequencies with potential energy distributions (Table S5), structural parameters and the HF/4-21G(*) constraints adopted in the data analysis of GED (Table S6), and the correlation matrix (Table S7) (19 pages). Ordering information is given on any current masthead page.

References and Notes

(1) A mesogen is a compound capable of forming liquid crystals.
(2) Brown, G. H.; Wolken, J. J. *Liquid Crystals and Biological Structures*; Academic Press: New York, 1979.
(3) de Gennes, P. G.; Prost, J. *The Physics of Liquid Crystals*, 2nd ed.; Oxford University Press: Oxford, 1993.
(4) Krigbaum, W. R.; Chatani, Y.; Barber, P. G. *Acta Crystallogr.* **1970**, *B26*, 97−102.
(5) Chebli, C.; Brisse, F. *Acta Crystallogr.* **1995**, *C51*, 1164−1167.
(6) Dong, R. Y.; Tomchuk, E.; Wade, C. G.; Visintainer, J. J.; Bock, E. *J. Chem. Phys.* **1977**, *66*, 4121−4125.
(7) Dianoux, A. J.; Ferreira, J. B.; Martins, A. F.; Giroud, A. M.; Volino, F. *Mol. Cryst. Liq. Cryst.* **1985**, *116*, 319−352.
(8) Ferreira, J. B.; Martins, A. F.; Galland, D.; Volino, F. *Mol. Cryst. Liq. Cryst.* **1987**, *151*, 283−301.
(9) Volino, F.; Galland, D.; Ferreira, J. B.; Dianoux, A. J. *J. Mol. Liquids* **1989**, *43*, 215−239.
(10) Kumanova, M. D. *Dokl. Bulg. Akad. Nauk* **1976**, *29*, 645−648.
(11) Kugler, S. *Acta Phys. Acad. Sci. Hung.* **1979**, *46*, 69−76.
(12) Perrin, H.; Bergès, J. *J. Physique* **1984**, *45*, 1947−1953.
(13) Schäfer, L.; Ewbank, J. D.; Siam, K.; Chiu, N.; Sellers, H. L. *Stereochemical Applications of Gas-Phase Electron Diffraction Part A-The Electron Diffraction Technique*; Hargittai, I., Hargittai, M., Eds.; VCH Publishers, Inc.: New York, 1988; Chapter 9.
(14) Konaka, S.; Kimura, M. Presented at the 13th Austin Symposium on Gas-Phase Molecular Structure, 12−14 March 1990; S21, The University of Texas, Austin, TX.
(15) Tsuboyama, A.; Murayama, A.; Konaka, S.; Kimura, M. *J. Mol. Struct.* **1984**, *118*, 351−354.
(16) Takeuchi, H.; Enmi, J.; Onozaki, M.; Egawa, T.; Konaka, S. *J. Phys. Chem.* **1994**, *98*, 8632−8635.
(17) Kimura, M.; Konaka, S.; Ogasawara, M. *J. Chem. Phys.* **1967**, *46*, 2599−2603.
(18) Tavard, C.; Nicolas, D.; Rouault, M. *J. Chim. Phys. Phys.-Chim. Biol.* **1967**, *64*, 540−554.
(19) Pulay, P. TX90 Program Description, University of Arkansas, Fayetteville, AR, 1990.
(20) Pulay, P.; Fogarasi, G.; Pang, F.; Boggs, J. E. *J. Am. Chem. Soc.* **1979**, *101*, 2550−2560.
(21) Fogarasi, G.; Zhou, X.; Taylor, P. W.; Pulay, P. *J. Am. Chem. Soc.* **1992**, *114*, 8191−8201.
(22) Dewar, M. J. S.; Zoebisch, E. G.; Heary, E. F.; Stewart, J. J. P. *J. Am. Chem. Soc.* **1985**, *107*, 3902.
(23) Stewart, J. J. P. *J. Comput. Chem.* **1989**, *10*, 209−220.
(24) Stewart, J. J. P. Quantum Chemistry Program Exchange, QCPE Bull. 9, Vol. 10, 1989.
(25) Maier, W.; Englert, G. *Z. Phys. Chem.* **1959**, *19*, 168−192.
(26) Amer, N. M.; Shen, Y. R. *J. Chem. Phys.* **1972**, *56*, 2654−2664.
(27) Schnur, J. M.; Hass, M.; Adair, W. L. *Phys. Lett.* **1972**, *41A*, 326−328.
(28) Bulkin, B. J.; Lok, W. B. *J. Phys. Chem.* **1973**, *77*, 326−330.
(29) Sakamoto, A.; Yoshino, K.; Kubo, U.; Inuishi, Y. *Jpn. J. Appl. Phys.* **1974**, *13*, 1691−1698.
(30) Gruger, A.; Romain, F. *J. Mol. Struct.* **1974**, *21*, 97−110.
(31) Shibata, K.; Kutsukake, M.; Takahashi, H.; Higashi, K. *Bull. Chem. Soc. Jpn.* **1976**, *49*, 406−409.
(32) Gruger, A.; Fillaux, J. *Spectrochim. Acta* **1972**, *28A*, 1253−1262.
(33) Balfour, W. J. *Spectrochim. Acta* **1983**, *39A*, 795−800.
(34) Owen, N. L.; Hester, R. E. *Spectrochim. Acta* **1969**, *25A*, 343−354.
(35) Coussens, B.; Pierloot, K.; Meier, R. J. *J. Mol. Struct.* **1992**, *259*, 331−344.
(36) Boggs, J. E. *Stereochemical Applications of Gas-Phase Electron Diffraction Part B.-Structural Information for Selected Classes of Compounds*; Hargittai, I., Hargittai, M., Eds.; VCH Publishers, Inc.: New York, 1988; Chapter 10; p 455−475.
(37) Kuchitsu, K.; Bartell, L. S. *J. Chem. Phys.* **1961**, *35*, 1945−1949.
(38) Kuchitsu, K. *Bull. Chem. Soc. Jpn.* **1967**, *40*, 505−510.
(39) Traetteberg, M.; Hilmo, I.; Hagen, K. *J. Mol. Struct.* **1977**, *39*, 231−239.
(40) Seip, H. M.; Seip, R. *Acta Chem. Scand.* **1973**, *27*, 4024−4027.
(41) Brunvoll, J.; Bohn, R. K.; Hargittai, I. *J. Mol. Struct.* **1985**, *129*, 81−91.
(42) Vilkov, L. V.; Sadova, N. I. *Stereochemical Applications of Gas-Phase Electron Diffraction Part B-Structural Information for Selected Classes of Compounds*; Hargittai, I., Hargittai, M., Eds.; VCH Publishers, Inc.: New York, 1988; Chapter 2; p 35−92.
(43) Exner, O.; Fruttero, R.; Gasso, A. *Struct. Chem.* **1989**, *1*, 417−421.
(44) Traetteberg, M.; Hilmo, I.; Abraham, R. J.; Ljunggren, S. *J. Mol. Struct.* **1978**, *48*, 395−405.